Published in final edited form as:
Cancer Res. 2009 March 1; 69(5): . doi:10.1158/0008-5472.CAN-08-3662.

Recapitulation of Pancreatic Neuroendocrine Tumors in Human Multiple Endocrine Neoplasia Type I (MEN1) Syndrome via Pdx1-directed Inactivation of *Men1*

H.-C. Jennifer Shen[1], **Mei He**[1], **Anathea Powell**[1], **Asha Adem**[1], **Dominique Lorang**[1], **Charles Heller**[1], **Amelia C. Grover**[1], **Kris Ylaya**[2], **Stephen M. Hewitt**[2], **Stephen J. Marx**[3], **Allen M. Spiegel**[4], and **Steven K. Libutti**[1]

[1]Tumor Angiogenesis Section, Surgery Branch, National Cancer Institute, Bethesda, Maryland 20892, USA

[2]Laboratory of Pathology, National Cancer Institute, Bethesda, Maryland 20892, USA

[3]Metabolic Diseases Branch, National Institute of Diabetes and Digestive and Kidney Diseases, National Institute of Health, Bethesda, Maryland 20892, USA

[4]Albert Einstein College of Medicine, Bronx, New York 10461, USA

Abstract

Multiple endocrine neoplasia type 1 (MEN1) is an autosomal syndrome caused by mutations in the MEN1 tumor suppressor gene. While the protein product of MEN1, menin, is ubiquitously expressed, somatic loss of the remaining wildtype *MEN1* allele results in tumors primarily in parathyroid, pituitary, and endocrine pancreas. To understand the endocrine specificity of the MEN1 syndrome, we evaluated biallelic loss of *Men1* by inactivating *Men1* in pancreatic progenitor cells utilizing the Cre-lox system. *Men1* deletion in progenitor cells that differentiate into exocrine and endocrine pancreas did not affect normal pancreas morphogenesis and development. However, mice having homozygous inactivation of the *Men1* in pancreas developed endocrine tumors with no exocrine tumor manifestation, recapitulating phenotypes seen in the MEN1 patients. In the absence of menin, the endocrine pancreas showed increase in cell proliferation, vascularity and abnormal vascular structures; such changes were lacking in exocrine pancreas. Further analysis revealed that these endocrine manifestations were associated with upregulation in VEGF expression in both human and mouse MEN1 pancreatic endocrine tumors. Together these data suggest the presence of cell-specific factors for menin and a permissive endocrine environment for MEN1 tumorigenesis in endocrine pancreas. Based on our analysis, we propose that menin's ability to maintain cellular and microenvironment integrity might explain the endocrine restrictive nature of the MEN1 syndrome.

Keywords

MEN1; pancreatic neuroendocrine tumor; VEGF; tumor suppressor gene; Pdx1

Requests for Reprints: Steven K. Libutti, M.D., Chief, Tumor Angiogenesis Section, Surgery Branch, National Cancer Institute, Building 10, Room 4W-5940, 10 Center Drive, Bethesda, MD 20892, Phone (301) 496-2195, Fax (301) 480-3825, Steven_Libutti@nih.gov.

Conflict of Interest Statement: None declared.

Introduction

Multiple endocrine neoplasia type 1 (MEN1; OMIM# 131100) is a dominant inherited syndrome caused by mutations in the *MEN1* tumor suppressor gene (1, 2). Patients with a family history of the MEN1 syndrome are predisposed to develop multiple endocrine tumors, primarily affecting parathyroid, anterior pituitary, and pancreatic islets. More than 95% of MEN1 patients develop clinical manifestations of the disorder by the fifth decade (3, 4), while the earliest occurrence has been reported at five years old (5). Consistent with Knudson's two-hit hypothesis for tumor suppressor genes (6), MEN1 monoclonal expansion is initiated when loss of heterozygosity (LOH) at 11q13 occurs in patients with inherited germ-line mutations of the *MEN1* gene (7–9). Additionally, somatic inactivation and LOH of the *MEN1* alleles have been reported in a variety of sporadic endocrine tumors, such as parathyroid adenomas and pancreatic insulinomas (10, 11). Mutations in the *MEN1* gene appear to be inactivating and no clear genotype-phenotype correlations have been established for mutations detected along the coding sequence of *MEN1* in both familial and sporadic tumors (12).

The protein product of *MEN1*, menin, does not display significant homology to any known family of proteins, and it has been described predominantly as a transcriptional regulator by interacting with nuclear proteins, such as JunD, NF-kB, Smad3, and FANCD2 (13, 14). Further biochemical studies have demonstrated that menin complexes with mixed-lineage leukemia (MLL) protein to regulate gene expression via chromatin modification in mouse embryonic fibroblast cells (15), bone marrow cells (16), as well as in human HeLa and leukemia cells (17, 18). Similar epigenetic regulation by menin has also been reported in endocrine tumors, where menin modulates histone methylation and expression of cyclin-dependent kinase inhibitors, p27 and p18 (19). More recently, menin has been implicated in the control of pancreatic β-cell growth during pregnancy (20). Together these studies have broadened our knowledge of menin's biochemical, physiological and pathological roles in both endocrine and non-endocrine contexts.

Utilizing mouse models to understand the human MEN1 syndrome has proven to be informative (21–23), perhaps due to the highly conserved genomic structures, nucleotide (89% identity) and amino acid (97% identity) sequences shared by mouse *Men1* and human *MEN1* genes (24, 25). Though mice deficient of both *Men1* alleles die *in utero* at E11.5–13.5 with developmental defects in multiple organs, mice heterozygous for *Men1* deletion develop endocrine tumors at maturity, similar to those found in human MEN1 patients (21, 22, 26). To circumvent the embryonic lethality, conditional inactivation of *Men1* has further confirmed that biallelic loss of menin in endocrine tissues can lead to the development of parathyroid adenoma (27), pancreatic insulinoma (28, 29), and pituitary prolactinoma (30). These observations are reminiscent of the tumor spectrum observed in mice with heterozygous germline deletion of *Men1*, as well as human MEN1 patients. While the generation of mouse models has effectively mimicked the human MEN1 syndrome, the mechanisms leading to the endocrine-specific tumorigenicity of the MEN1 syndrome remain to be elucidated.

Based on published biochemical and genetic analyses on *Men1*, we postulated that tumorigenicity of the MEN1 syndrome may be explained by cell-specific co-factors for menin because expression of menin is not restricted to endocrine tissues (25, 31), while most manifestations of MEN1 essentially are endocrine specific. To test this hypothesis, we chose to selectively inactivate *Men1* in pancreatic progenitor cells during embryogenesis, such that *Men1* alleles are deleted in exocrine and endocrine cells of the pancreas. Our aim was to determine whether complete loss of menin in cells of pancreatic lineage leads to tumorigenesis only in MEN1-affected endocrine tissues, or in pancreatic exocrine tissues as

well. Here we describe that similar to MEN1 patients with neuroendocrine tumors, mice completely deficient of *Men1* in both endocrine and exocrine pancreas developed only pancreatic endocrine tumors, supporting the hypothesis that cell-specific factors exist to explain the tissue-selective tumorigenicity of the MEN1 syndrome. We further provide evidence demonstrating that alterations in the endocrine microenvironment, such as upregulation in vascular endothelial growth factor (VEGF) expression, are involved in developing pancreatic endocrine tumors resulting from the loss of menin. Together, these findings suggest that cell-specific factors are involved MEN1 pancreatic tumorigenesis and that a permissive microenvironment is essential in this process.

Materials and Methods

Animals and Genotyping

Mice carrying the *Men1* alleles flanked by loxP sites (Men1 f/f or Men1 ΔN/ΔN) in (29) were crossed with Pdx1-Cre transgenic mice (a kind gift from D. Melton, (32)) to generate Pdx1-Cre;Men1 f/+ heterozygous mice in mixed FVB;129Sv background. Pdx1-Cre;Men1 f/+ heterozygous mice were bred to generate Pdx1-Cre;Men1 f/f, Pdx1-Cre;Men1 f/+, and control genotypes, Pdx1-Cre, and Men1 f/f. All mice were genotyped by PCR using DNA isolated from tail snip, with an annealing temperature of 55°C for both *Pdx1-Cre* and *Men1* floxed alleles. Primers for Pdx1-Cre (forward: 5'-TTGAAACAAGTGCAGGTGTTCG; reverse: 5'- CCTGAAGATATAGAAGATAATCG), and for *Men1* floxed alleles (forward: 5'- ATTGATGAGACCGCAAGGAC; reverse: 5'- GTCCTGGAGAGCAGAACCTTG) were utilized. The PCR conditions for detecting deleted *Men1* alleles have been described (22).

Western blotting

Total pancreatic protein lysate was harvested by sonicating pancreas on ice in RIPA buffer (Pierce, Rockford, IL) containing 1× Complete Protease Inhibitor Cocktail (Roche, Nutley, NJ). Protein concentration was determined with the Quick Start Bradford Protein Assay (Bio-Rad Laboratories, Hercules, CA). Protein (15 or 30ug/lane) was resolved on 4–12% NuPAGE gel with 1× MOPS running buffer (Invitrogen, Carlsbad, CA), followed by transferring to nitrocellulose membranes using iBlot (Invitrogen, Carlsbad, CA). Membranes were blocked in 5% non-fat milk (Bio-Rad Laboratories, Hercules, CA) in 0.1%Tween-20/PBS, and sequentially incubated with primary and secondary antibodies with washes in between using 0.1%Tween-20/PBS. Protein detection was performed with Amersham ECL Western Blotting Detection Reagents (GE Healthcare, Waukesha, WI). Primary antibodies used were rabbit anti-menin (1:1000, Bethyl, Montgomery, TX), and goat anti-actin (1:200, Santa Cruz Biotechology Inc., Santa Cruz, CA). Secondary antibodies used were goat anti-rabbit IgG-horseradish peroxidase (HRP), and rabbit anti-goat IgG-HRP (Millipore, Billerica, MA).

Insulin and Glucose Measurements

For insulin and glucose measurements, mice underwent a 24 hour fast prior to collecting whole blood via orbital or mandible bleed. Blood glucose was measured using a glucometer (Ascensia Contour, Bayer HealthCare, Mishawaka, IN). Plasma collected using 0.5M EDTA as anticoagulant was measured for insulin levels with the Ultrasensitive Mouse Insulin ELISA kit (Mercodia Inc., Winston Salem, NC) according to the manufacturer's instructions.

Histological Analysis

FITC-lectin perfusion to visualize the vasculature was performed as described (33). Briefly mice were injected intravenously via tail vein with 50ug of FITC-labeled lectin (*Lycopersicon esculentum*, Vector Laboratories, Burlingame, CA), which was allowed to circulate for 3 minutes. Then mice were euthanized via cervical dislocation, and their pancreas was removed. The pancreatic tissue was processed for both frozen histological analysis by embedding tissues in Tissue-Tek OCT freezing medium, and for formalin-fixed paraffin embedding (FFPE). For all immuno-staining experiments described below, appropriate positive and negative controls were run concurrently for all the applied antisera on the adjacent pancreas sections.

Frozen (10–20um) and FFPE sections (5um) of mouse pancreas were routinely stained with Mayer's hemotoxylin and eosin (H&E) for histopathological analysis. For immuno-histochemical staining of VEGF, a goat anti-mouse VEGF (1:50, R&D Systems, Minneapolis, MN) or a monoclonal antibody against human VEGF (clone VG1, 1:50, Thermo Fisher Scientific, Fremont, CA) was used. Sections were counterstained in Mayer's hemotoxylin, mounted, and photographed using a Zeiss microscope.

For immuno-staining of FITC-lectin injected pancreas, frozen sections were briefly fixed in 4% paraformaldehyde, washed in PBS, and incubated in blocking buffer (5% normal goat serum/2.5% BSA in PBS). Primary antibodies were diluted in 0.5× blocking buffer: guinea pig anti-swine insulin (1:500, DAKO, Carpinteria, CA), rabbit anti-human gastrin (1:500, Novocastra/DAKO, Carpinteria, CA), rabbit anti-human chromogranin A (ready to use, Invitrogen, Carlsbad, CA), rabbit anti-synaptophysin (1:50, Diagnostic BioSystems, Pleasanton, CA), sheep anti-human CD31 (1:30, R&D Systems, Minneapolis, MN), and monoclonal rabbit anti-human Ki67 (1:500, Thermo Fisher Scientific, Fremont, CA). Sections were incubated with primary antibody overnight at 4°C in a humidified chamber followed by brief washes in PBS. Secondary antibodies (Invitrogen, Carlsbad, CA) Alexa Fluor 594 or 633-conjugated anti-rabbit (1:500), Alexa Fluor 594 or 633-conjugated anti-guinea pig (1:200), or Alexa Fluor 488-conjugated anti-sheep (1:200) were applied to sections. After incubation at room temperature for one hour, the fluorescently stained sections were washed several times in PBS, cover slipped using mounting medium with DAPI (Vector Laboratories, Burlingame, CA) and visualized using either a Zeiss Axiovert fluorescence microscope or a Zeiss LSM 510 Laser Scanning confocal microscope (Carl Zeiss MicroImaging, Thornwood, NY).

For quantitative analysis of immuno-fluorescent images and islet areas within the pancreas, multiple images from the same animals were analyzed using the Zeiss imaging software AxioVision (Carl Zeiss MicroImaging, Thornwood, NY). Application specific macros written by Zeiss support were applied to each image to allow unbiased quantification of the positive signals. Densitometry for each of the images were additionally evaluated and controlled for staining variability among different samples. Human neuroendocrine tumor images were "mosaic" images consisting of a quilt of four consecutive low powered fields stitched together using the same imaging software as described (34).

VEGF ELISA

Mouse VEGF protein was measured using Quantikine mouse VEGE immunoassay according to manufacturer's protocols (R&D Systems, Minneapolis, MN).

In Vivo Treatment study

Sunitinib was suspended in an aqueous solution of 0.5% carboxymethylcellulose and 0.25% Tween 80 as described previously (34). Age, weight, and sex-matched mice for each

genotype, Men1 f/f and Pdx1-Cre;Men1 f/f, were treated with sunitinib (20mg/kg of weight, (35) or vehicle via oral gavage daily for 3 months. Mice began treatment at an average age of 3-month old. During the treatment period, body weight for each animal was monitored for treatment toxicity and for calculating sunitinib dosing monthly. For each animal, images of all islets in each section were captured for quantitative analysis. All animal experiments were conducted in accordance with NIH and AALAC approved protocols and guidelines.

Human Tissue Samples

Normal pancreas as well as MEN1 pancreatic neuroendocrine tumors were obtained from patients under NIH IRB approved protocols. After surgical removal, the samples were flash frozen in liquid nitrogen and stored at −80°C, or formalin-fixed for paraffin embedding. Frozen pancreas were embedded in Optimal Cryo Temperature (OCT) compound (Tissue Tek II, Miles, Elkhart, ID) on dry ice before being sectioned to 8–10 μm thickness for histologic analysis. Frozen sections from two different MEN1 patients were used for immuno-fluorescent staining of insulin, CD31, and chromogranin A. These two patients were operated on for tumor size and/or metastasis, and tumors were positive for general pancreatic neuroendocrine tumor markers (chromogranin A and synaptophysin). Additional pancreatic neuroendocrine tumors from four different MEN1 patients (two insulinomas and two gastrinomas) were used for immuno-histochemial staining of VEGF on their FFPE tumor sections. Sections of normal and neuroendocrine tumors were blindly evaluated and identified by pathologist (S.M.H.).

Statistical Analysis

Statistical analysis was performed using GraphPad InStat v.3.05, GraphPad Prism v.4.02, and Microsoft Excel. Imaging quantification data were analyzed with a Mann-Whitney non-parametric test, except percentage of islet area per pancreas section (Figure 1C) was evaluated with two-tailed student t-test. Plasma insulin levels, blood glucose level, and VEGF ELISA were evaluated with one-way ANOVA with multiple comparisons testing. A p value less than (<) 0.05 was considered statistically significant.

Results

Loss of menin in pancreatic progenitor cells does not affect normal pancreas development, but leads to increase in cell proliferation only in endocrine pancreas

To further understand the tissue-specific role of *MEN1* in tumorigenesis, we generated a conditional knockout mouse model to evaluate the loss of *Men1* in both exocrine and endocrine pancreas cells using a Cre-loxP system. Transgenic mice expressing cre recombinase from the pancreatic and duodenal homeobox 1 (Pdx1) promoter allowed target gene deletion in all pancreatic endocrine and exocrine cells due to Pdx1-Cre expression in pancreatic progenitor cells (32). The Pdx1-Cre transgenic mice bred with mice whose *Men1* alleles are flanked by loxP sites from exons 3 to 8 (Men1f/f, (22)) gave expected Mendelian frequencies for all genotypes (supplementary data – Table 1). Laser capture microdissection of genomic DNA from pancreatic endocrine and exocrine cells showed the expected deletion of *Men1* alleles in all pancreatic cells of Pdx1-Cre;Men1 f/f animals (Figure 1A, bottom panel). Furthermore, using total pancreatic lysate, we confirmed a significant reduction of menin protein expression in Pdx1-Cre;Men1 f/f homozygous mice (Figure 1B). Together, these results demonstrated that Pdx1-Cre mediated loss of menin in the pancreas is not lethal to embryogenesis and does not affect normal pancreas development.

Histopathological analysis of pancreatic tissues at early time points (2–3 months) showed normal exocrine glandular components and endocrine islets in Pdx1-Cre (n=1), Men1 f/f (n=5), Pdx1-Cre;Men1 f/+ (n=10), and Pdx1-Cre;Men1 f/f (n=6) animals (supplementary

data A). Since *Men1* deletion has been shown to lead to increased in β-cell proliferation (36), we tested whether or not loss of *Men1* in pancreatic progenitor cells would result in an increase in proliferation potential in both endocrine and exocrine cells of pancreas. We elected to use Ki-67 as the cell proliferation marker for all pancreatic cells, and insulin as a marker for endocrine cells by immuno-fluorescent staining (Figure 1C and supplementary data B). As expected, Pdx1-Cre;Men1 f/f mice indeed had more proliferating cells within their islets, when compared to age-matched control genotype Men1 f/+ mice (Figure 1D). However, although deletion of *Men1* alleles was confirmed by PCR in exocrine cells of Pdx1-Cre;Men1 f/f pancreas (Figure 1A), no significant difference in the number of proliferating cells was detected in non-endocrine cells outside islets (Figure 1D).

Inactivation of Men1 in exocrine and endocrine cells of pancreas leads exclusively to endocrine tumor development in Pdx1-Cre;Men1 f/f mice

Further characterization of older Pdx1-Cre;Men1 f/f mice showed enlarged and hyperplastic islets as early as 5–6 months of age, and these mice exhibited progression to insulinoma by 10–12 months of age (Figure 2A). Gastrinoma was not observed in Pdx1-Cre;Menf f/f pancreas at 12+ month of age (n=5, data not shown), even though gastrinoma has been reported in a different mouse model of MEN1 (21). Insulinomas were filled with blood islands or lacunae, and characterized by disorganized tumor cells with aberrant nuclei (Figure 2A, right lower panel). Yet, no histological abnormality was observed in the exocrine tissues of Pdx1-Cre;Men1 f/f animals. Consistent with the development of hyperplastic islets and insulinomas, the Pdx1-Cre;Men1 f/f mice had elevated plasma insulin levels that were significantly different from the control genotypes (Pdx1-Cre and Men1 f/f) starting at 5 months of age and persisting throughout their lifetime (Figure 2B). Notably the 16-month old Pdx1-Cre;Men1 f/+ mice began to display elevated plasma insulin levels, suggesting the development of hyperplastic islets due to the loss of the other wildtype *Men1* allele, as has been described (21–23). As expected, elevated insulin levels were accompanied by a decrease in fasting blood glucose starting at 10 month of age (supplementary data C). Moreover, the Pdx1-Cre;Men1 f/f mice had a shorter life span, as 50% of them died at approximately 14 months of age, while more than 50% of the control genotypes lived beyond 24 months (Figure 2C).

VEGF contributes to the abnormal islet vasculature and the insulinomas developed in Pdx1-Cre;Men1 f/f mice

To investigate the reason why complete loss of Men1 in the pancreas only resulted in an endocrine phenotype in Pdx1-Cre;Men1 f/f mice, we speculated that, in addition to cell-specific factors, pancreatic endocrine tissues provide a more permissive environment for tumor development. Since it is well-established that vascular changes and angiogenesis are critical steps during tumor progression (37, 38), we hypothesized that loss of *Men1* alters islet vasculature and correlates with the insulinomas developed in Pdx1-Cre;Men1 f/f mice. To visualize pancreatic vasculature, mice were intravenously injected with FITC-lectin prior to euthanasia. By immuno-fluorescent staining with anti-insulin antibodies, we were able to distinguish endocrine islets from exocrine tissues of the pancreas (Figure 3A). Quantitative analyses of immuno-fluorescent images of control and Pdx1-Cre;Men1 f/f pancreas showed a significant increase in islet vascularity in Pdx1-Cre;Men1 f/f mice as early as 3-month old and at 10 months of age (Figure 3B). In addition, the vasculature of some Pdx1-Cre;Men1 f/f islets exhibited structural abnormalities, as indicated by dilation of blood vessels and intense tortuosity present in both 3-month and 12-month old animals (Figure 3C). These changes in islet vascularity appeared to pre-date the development of endocrine tumors. At all time points analyzed, we did not detect differences in vascular density and vessel morphology in exocrine tissues between control and Pdx1-Cre;Men1 f/f pancreas (supplementary data D).

Because VEGF is a central regulator of angiogenesis, we next performed VEGF ELISA to determine if the vascular alterations in Pdx1-Cre;Men1 f/f islets was due to changes in VEGF expression. Indeed, elevated pancreatic VEGF protein was detected in mice as early as 3 months of age, and was significantly different between control and Pdx1-Cre;Men1 f/f homozygous mice at 12 months of age (Figure 4A). Immuno-histochemical staining using a VEGF antibody further demonstrated that elevation of VEGF expression predominantly localized in the endocrine tissues of pancreas (Figure 4B). To confirm that VEGF plays an important role during insulinoma progression in Pdx1-Cre;Men1 f/f mice, we elected to inhibit VEGF signaling with sunitinib, a small-molecule tyrosine kinase inhibitor that is known to inhibit all VEGF receptors (39). A cohort of sex and weight-matched Men1 f/f and Pdx1-Cre;Men1 f/f mice averaged 3-month old were treated with vehicle or sunitinib via daily oral gavage for 3 months. At the end of treatment, the pancreas of these mice was subjected to immuno-fluorescent imaging analysis for islet cell proliferation and islet vascularity. The number of animals and images analyzed were included in supplementary data - Table 2. As indicated by percentage of Ki-67 positive cells within each islet, a significant reduction in cell proliferation was observed in Pdx1-Cre;Men1 f/f animals treated with sunitinib, but not in sunitinib-treated Men1 f/f animals (Figure 5A and 5B). Similarly, Pdx1-Cre;Men1f/f mice treated with sunitinib exhibited a significant decrease in islet vascularity, while no differences in islet vascularity was observed between vehicle and sunitinib treated Men1 f/f mice (Figure 5C and 5D). We also determined pancreatic VEGF protein expression and found no differences between vehicle and treatment group for each genotype (supplementary data E). This result is not surprising as sunitinib functions to inhibit VEGF signaling, but not VEGF secretion. Together these data suggest that VEGF signaling is a critical pathway involved in tumors developed in this mouse model of MEN1.

Human MEN1 pancreatic neuroendocrine tumors displayed similar characteristics as endocrine tumors developed in mice deficient of menin in pancreas

Similar to MEN1 patients with pancreatic neuroendocrine tumors, the Pdx1-Cre;Men1 f/f homozygous mice progressively developed insulinomas due to inactivation of menin in pancreas. To evaluate if our mouse model of MEN1 recapitulates the human MEN1 syndrome, we utilized immuno-fluorescent staining to analyze human MEN1 neuroendocrine tumors for cell proliferation and vascular morphology, parameters used to establish our mouse model. As shown in Figure 6A, in the “normal” portion of the pancreas that was not involved in tumor, only a few proliferating cells were detected in islets; in contrast to the neuroendocrine tumors containing many Ki-67 positive proliferating cells (Figure 6A). Using a CD31 antibody to identify blood vessels, we further demonstrated hypervascularity and dilatation of vessels within the MEN1 neuroendocrine tumors from patients (Figure 6B). Moreover, immuno-histochemical analysis revealed abundant VEGF expression in all MEN1 neuroendocrine tumors tested (n=4). While positive VEGF expression was detected also in islets of the adjacent normal pancreas, VEGF expression is absent in the exocrine pancreas (Figure 6C). The similarities shared between the Pdx1-Cre;Men1 mouse model and the human MEN1 neuroendocrine tumors supports that our mouse model represents a powerful tool for investigating the molecular mechanisms related to MEN1 tumorigenesis in patients.

Discussion

In the present study, we aimed to elucidate the tissue-specific nature of the lesions associated with the MEN1 syndrome utilizing a mouse model where menin is deleted in progenitor cells that gave rise to both exocrine and endocrine pancreas during development. We revealed that pancreatic progenitor cells lacking menin were able to differentiate into normal endocrine and exocrine pancreas. However, adult endocrine cells lacking menin

developed tumors, in contrast to adult exocrine cells, which remained phenotypically normal in the absence of menin. In other words, we established that loss of menin is sufficient to cause endocrine tumorigenesis but insufficient to initiate exocrine tumorigenesis in the pancreas. This novel observation supports the hypothesis that cell-specific factors must exist to explain the tissue specific tumorigenesity of the MEN1 syndrome. In addition, we demonstrated for the first time in literature that upregulation in VEGF expression is associated with MEN1 pancreatic neuroendocrine tumors developed in human and mice. Together, these findings imply that cell-specific modulators for menin and alterations in microenvironment are crucial for MEN1 tumorigenesis in the endocrine pancreas. Therefore, the tissue restricted nature of MEN1 lesions may reside within not only the cellular context, but also the surrounding microenvironment of the endocrine cells affected in MEN1 syndrome.

The major difference distinguishing our conditional murine model of MEN1 from the previously described MEN1 models of insulinomas (28–30) is that all pancreatic cells are deficient of menin in our mice. Not previously described in literature, we demonstrated that menin is not required for pancreatic morphogenesis and differentiation during development. We further revealed that loss of menin in exocrine cells does not result in histological and functional abnormalities in the exocrine pancreas. Notably, loss of menin led to an increased in cell proliferation and tumor development in endocrine pancreas, and those phenotypes was not observed in exocrine pancreas. This is a significant observation in that deletion of *Men1* in the same progenitor cells of pancreatic lineage only leads to tumor formation in cells that differentiate into pancreatic endocrine cells. Our findings were similar to a report where homozygous loss of menin in hepatocytes is well-tolerated without neoplasia (40). Collectively these murine models of *Men1* imply that the endocrine restricted tumor pattern seen in the MEN1 syndrome is likely due to cell- or tissue-specific factors for menin, because expression of menin is ubiquitous (25, 31). While the identities of endocrine cell-specific factors for menin remain a mystery, it has been speculated that the endocrine tumor bias in the MEN1 syndrome results from a requirement of menin to maintain expression of cyclin-kinase inhibitors, such as p27 and p18, in endocrine cells (19, 41, 42). Yet, it does not exclude the possibility that other protective molecules and mechanisms exist in non-endocrine tissues in the absence of menin. Therefore, our model system will serve as a valuable tool to test these hypotheses, and may be utilized to uncover potential target genes and co-factors for menin.

Another plausible explanation for the tumorgenicity of the MEN1 syndrome might reside in the unique characteristics of the endocrine microenvironment. It has been established that endocrine pancreatic β-cells require endothelial signals for differentiation and function (43), and that distinctly different extracellular proteins are detected in the basement membranes of endocrine and exocrine cells (44). Recently, it has been shown that endocrine β-cells, in contrast to exocrine pancreatic cells, do not produce a basement membrane of extracellular matrix. Instead, β-cells use VEGF to attract endothelial cells to form basement membranes next to them, which contain signals to promote β-cell proliferation and insulin secretion (45). In the present study, we demonstrated that the insulinomas developed due to loss of menin are associated with an increase in VEGF expression, and that blocking VEGF signaling with sunitinib was sufficient to inhibit islet cell proliferation in our Pdx1-Cre;Men1 f/f animals. Similarly, inhibiting VEGF with a monoclonal VEGF antibody has been shown to result in a decrease in tumor volume in a pituitary mouse model of MEN1 (46). The significance of VEGF in contributing to tumors developed in our model ought to be further validated using specific VEGF inhibitors since sunitinib is also known to block other tyrosine kinase signaling pathways (39, 47). However, our data, together with the published literature, support a critical role of VEGF in vascularization and growth of MEN1-associated tumors. Analysis of other MEN1-associated endocrine tumors, such as

parathyroid adenoma, might provide further evidence to underline the future potential for an anti-VEGF therapy in MEN1 endocrine neoplasms.

It is also important to note that our molecular and histological analysis on a vascular phenotype of MEN1 pancreatic neuroendocrine tumors is the first one in literature that links VEGF in driving tumor formation following *Men1* deletion. While a direct functional relationship between menin and VEGF is yet to be determined, angiogenesis and VEGF have been shown to be critical in a non-MEN1 model of insulinoma (48, 49). Thus, it would be of great interest to learn whether menin loss is involved in this model system. In addition, although angiogenesis and VEGF are the focus of this study, possibilities exist that loss of menin may lead to other microenvironment changes, allowing the endocrine islets to be more permissive for tumor development. Based on our data using both human and mouse pancreatic neuroendocrine tumors, we speculate that islet cells lacking menin use VEGF to induce endothelial cells to create a permissive islet microenvironment for the growth of naturally occurring MEN1 tumors. However, further molecular studies will be required to elucidate the functional relationship between menin and VEGF, and to determine if the absence of exocrine lesions in MEN1 patients and in our Pdx1-Cre;Men1 f/f mice might be due to the differences in extracellular signals generated by cells deficient for menin.

Based on our mouse model of MEN1 described here, we propose that the endocrine tissue restrictive nature of the MEN1 syndrome is due to both cellular factors for menin and the permissive endocrine microenvironment. It is thus possible that menin mediates tumor suppression by maintaining cellular and microenvironment integrity. Our mouse model of MEN1 serves as an ideal system to further decipher cell-specific factors for menin, and to investigate the significance of microenvironment alterations in MEN1 tumorigenesis. Comparative analysis of both exocrine and endocrine tissues lacking menin will enhance our understanding of the MEN1 syndrome, and provide vital clues for the presence of protective mechanisms in tissues not affected by the loss of *Men1*. The use of mouse models may ultimately derive important insights into the biology of the disease, which may guide toward novel therapeutics for the MEN1 patients.

Supplementary Material

Refer to Web version on PubMed Central for supplementary material.

Acknowledgments

The authors thank Dr. F. Collins for his insightful comments and participation during development of this project. We also thank Drs. A. Tandle and M. Kwon for useful discussions and Drs. S. Agarwal and S. Chandrasekharappa for helpful advice

Financial Support: This research was supported by funds from the Intramural Research Program of the National Institutes of Health, National Cancer Institute and National Institute of Diabetes and Digestive Diseases.

References

1. Chandrasekharappa SC, Guru SC, Manickam P, et al. Positional cloning of the gene for multiple endocrine neoplasia-type 1. Science. 1997; 276:404–407. [PubMed: 9103196]
2. Lemmens I, Van de Ven WJ, Kas K, et al. Identification of the multiple endocrine neoplasia type 1 (MEN1) gene. The European Consortium on MEN1. Hum Mol Genet. 1997; 6:1177–1183. [PubMed: 9215690]
3. Marx S, Spiegel AM, Skarulis MC, Doppman JL, Collins FS, Liotta LA. Multiple endocrine neoplasia type 1: clinical and genetic topics. Ann Intern Med. 1998; 129:484–494. [PubMed: 9735087]

4. Trump D, Farren B, Wooding C, et al. Clinical studies of multiple endocrine neoplasia type 1 (MEN1). Qjm. 1996; 89:653–669. [PubMed: 8917740]
5. Stratakis CA, Schussheim DH, Freedman SM, et al. Pituitary macroadenoma in a 5-year-old: an early expression of multiple endocrine neoplasia type 1. J Clin Endocrinol Metab. 2000; 85:4776–4780. [PubMed: 11134142]
6. Knudson AG Jr. Mutation and cancer: statistical study of retinoblastoma. Proc Natl Acad Sci U S A. 1971; 68:820–823. [PubMed: 5279523]
7. Guru SC, Manickam P, Crabtree JS, Olufemi SE, Agarwal SK, Debelenko LV. Identification and characterization of the multiple endocrine neoplasia type 1 (MEN1) gene. J Intern Med. 1998; 243:433–439. [PubMed: 9681840]
8. Ludwig L, Schleithoff L, Kessler H, Wagner PK, Boehm BO, Karges W. Loss of wild-type MEN1 gene expression in multiple endocrine neoplasia type 1-associated parathyroid adenoma. Endocr J. 1999; 46:539–544. [PubMed: 10580746]
9. Valdes N, Alvarez V, Diaz-Cadorniga F, et al. Multiple endocrine neoplasia type 1 (MEN1): LOH studies in a affected family and in sporadic cases. Anticancer Res. 1998; 18:2685–2689. [PubMed: 9703929]
10. Heppner C, Kester MB, Agarwal SK, et al. Somatic mutation of the MEN1 gene in parathyroid tumours. Nat Genet. 1997; 16:375–378. [PubMed: 9241276]
11. Wang EH, Ebrahimi SA, Wu AY, Kashefi C, Passaro E Jr, Sawicki MP. Mutation of the MENIN gene in sporadic pancreatic endocrine tumors. Cancer Res. 1998; 58:4417–4420. [PubMed: 9766672]
12. Lemos MC, Thakker RV. Multiple endocrine neoplasia type 1 (MEN1): analysis of 1336 mutations reported in the first decade following identification of the gene. Hum Mutat. 2008; 29:22–32. [PubMed: 17879353]
13. Agarwal SK, Kennedy PA, Scacheri PC, et al. Menin molecular interactions: insights into normal functions and tumorigenesis. Horm Metab Res. 2005; 37:369–374. [PubMed: 16001329]
14. Balogh K, Racz K, Patocs A, Hunyady L. Menin and its interacting proteins: elucidation of menin function. Trends Endocrinol Metab. 2006; 17:357–364. [PubMed: 16997566]
15. Hughes CM, Rozenblatt-Rosen O, Milne TA, et al. Menin associates with a trithorax family histone methyltransferase complex and with the hoxc8 locus. Mol Cell. 2004; 13:587–597. [PubMed: 14992727]
16. Chen YX, Yan J, Keeshan K, et al. The tumor suppressor menin regulates hematopoiesis and myeloid transformation by influencing Hox gene expression. Proc Natl Acad Sci U S A. 2006; 103:1018–1023. [PubMed: 16415155]
17. Yokoyama A, Somervaille TC, Smith KS, Rozenblatt-Rosen O, Meyerson M, Cleary ML. The menin tumor suppressor protein is an essential oncogenic cofactor for MLL-associated leukemogenesis. Cell. 2005; 123:207–218. [PubMed: 16239140]
18. Yokoyama A, Wang Z, Wysocka J, et al. Leukemia proto-oncoprotein MLL forms a SET1-like histone methyltransferase complex with menin to regulate Hox gene expression. Mol Cell Biol. 2004; 24:5639–5649. [PubMed: 15199122]
19. Karnik SK, Hughes CM, Gu X, et al. Menin regulates pancreatic islet growth by promoting histone methylation and expression of genes encoding p27Kip1 and p18INK4c. Proc Natl Acad Sci U S A. 2005; 102:14659–14664. [PubMed: 16195383]
20. Karnik SK, Chen H, McLean GW, et al. Menin controls growth of pancreatic beta-cells in pregnant mice and promotes gestational diabetes mellitus. Science. 2007; 318:806–809. [PubMed: 17975067]
21. Bertolino P, Tong WM, Galendo D, Wang ZQ, Zhang CX. Heterozygous Men1 mutant mice develop a range of endocrine tumors mimicking multiple endocrine neoplasia type 1. Mol Endocrinol. 2003; 17:1880–1892. [PubMed: 12819299]
22. Crabtree JS, Scacheri PC, Ward JM, et al. A mouse model of multiple endocrine neoplasia, type 1, develops multiple endocrine tumors. Proc Natl Acad Sci U S A. 2001; 98:1118–1123. [PubMed: 11158604]
23. Loffler KA, Biondi CA, Gartside M, et al. Broad tumor spectrum in a mouse model of multiple endocrine neoplasia type 1. Int J Cancer. 2007; 120:259–267. [PubMed: 17044021]

24. Bassett JH, Rashbass P, Harding B, Forbes SA, Pannett AA, Thakker RV. Studies of the murine homolog of the multiple endocrine neoplasia type 1 (MEN1) gene, men1. J Bone Miner Res. 1999; 14:3–10. [PubMed: 9893060]
25. Guru SC, Crabtree JS, Brown KD, et al. Isolation, genomic organization, and expression analysis of Men1, the murine homolog of the MEN1 gene. Mamm Genome. 1999; 10:592–596. [PubMed: 10341092]
26. Bertolino P, Radovanovic I, Casse H, Aguzzi A, Wang ZQ, Zhang CX. Genetic ablation of the tumor suppressor menin causes lethality at mid-gestation with defects in multiple organs. Mech Dev. 2003; 120:549–560. [PubMed: 12782272]
27. Libutti SK, Crabtree JS, Lorang D, et al. Parathyroid gland-specific deletion of the mouse Men1 gene results in parathyroid neoplasia and hypercalcemic hyperparathyroidism. Cancer Res. 2003; 63:8022–8028. [PubMed: 14633735]
28. Bertolino P, Tong WM, Herrera PL, Casse H, Zhang CX, Wang ZQ. Pancreatic beta-cell-specific ablation of the multiple endocrine neoplasia type 1 (MEN1) gene causes full penetrance of insulinoma development in mice. Cancer Res. 2003; 63:4836–4841. [PubMed: 12941803]
29. Crabtree JS, Scacheri PC, Ward JM, et al. Of mice and MEN1: Insulinomas in a conditional mouse knockout. Mol Cell Biol. 2003; 23:6075–6085. [PubMed: 12917331]
30. Biondi CA, Gartside MG, Waring P, et al. Conditional inactivation of the MEN1 gene leads to pancreatic and pituitary tumorigenesis but does not affect normal development of these tissues. Mol Cell Biol. 2004; 24:3125–3131. [PubMed: 15060136]
31. Stewart C, Parente F, Piehl F, et al. Characterization of the mouse Men1 gene and its expression during development. Oncogene. 1998; 17:2485–2493. [PubMed: 9824159]
32. Gu G, Dubauskaite J, Melton DA. Direct evidence for the pancreatic lineage: NGN3+ cells are islet progenitors and are distinct from duct progenitors. Development. 2002; 129:2447–2457. [PubMed: 11973276]
33. Thurston G, Baluk P, Hirata A, McDonald DM. Permeability-related changes revealed at endothelial cell borders in inflamed venules by lectin binding. Am J Physiol. 1996; 271:H2547–H2562. [PubMed: 8997316]
34. Blansfield JA, Caragacianu D, Alexander HR 3rd, et al. Combining Agents that Target the Tumor Microenvironment Improves the Efficacy of Anticancer Therapy. Clin Cancer Res. 2008; 14:270–280. [PubMed: 18172279]
35. Chow LQ, Eckhardt SG. Sunitinib: from rational design to clinical efficacy. J Clin Oncol. 2007; 25:884–896. [PubMed: 17327610]
36. Schnepp RW, Chen YX, Wang H, et al. Mutation of tumor suppressor gene Men1 acutely enhances proliferation of pancreatic islet cells. Cancer Res. 2006; 66:5707–5715. [PubMed: 16740708]
37. Carmeliet P. Angiogenesis in life, disease and medicine. Nature. 2005; 438:932–936. [PubMed: 16355210]
38. Folkman J, Watson K, Ingber D, Hanahan D. Induction of angiogenesis during the transition from hyperplasia to neoplasia. Nature. 1989; 339:58–61. [PubMed: 2469964]
39. Mendel DB, Laird AD, Xin X, et al. In vivo antitumor activity of SU11248, a novel tyrosine kinase inhibitor targeting vascular endothelial growth factor and platelet-derived growth factor receptors: determination of a pharmacokinetic/pharmacodynamic relationship. Clin Cancer Res. 2003; 9:327–337. [PubMed: 12538485]
40. Scacheri PC, Crabtree JS, Kennedy AL, et al. Homozygous loss of menin is well tolerated in liver, a tissue not affected in MEN1. Mamm Genome. 2004; 15:872–877. [PubMed: 15672591]
41. Bai F, Pei XH, Nishikawa T, Smith MD, Xiong Y. p18Ink4c, but not p27Kip1, collaborates with Men1 to suppress neuroendocrine organ tumors. Mol Cell Biol. 2007; 27:1495–1504. [PubMed: 17145768]
42. Franklin DS, Godfrey VL, O'Brien DA, Deng C, Xiong Y. Functional collaboration between different cyclin-dependent kinase inhibitors suppresses tumor growth with distinct tissue specificity. Mol Cell Biol. 2000; 20:6147–6158. [PubMed: 10913196]
43. Lammert E, Gu G, McLaughlin M, et al. Role of VEGF-A in vascularization of pancreatic islets. Curr Biol. 2003; 13:1070–1074. [PubMed: 12814555]

44. Jiang FX, Naselli G, Harrison LC. Distinct distribution of laminin and its integrin receptors in the pancreas. J Histochem Cytochem. 2002; 50:1625–1632. [PubMed: 12486084]
45. Nikolova G, Jabs N, Konstantinova I, et al. The vascular basement membrane: a niche for insulin gene expression and Beta cell proliferation. Dev Cell. 2006; 10:397–405. [PubMed: 16516842]
46. Korsisaari N, Ross J, Wu X, et al. Blocking vascular endothelial growth factor-A inhibits the growth of pituitary adenomas and lowers serum prolactin level in a mouse model of multiple endocrine neoplasia type 1. Clin Cancer Res. 2008; 14:249–258. [PubMed: 18172277]
47. Fabian MA, Biggs WH 3rd, Treiber DK, et al. A small molecule-kinase interaction map for clinical kinase inhibitors. Nat Biotechnol. 2005; 23:329–336. [PubMed: 15711537]
48. Hanahan D. Heritable formation of pancreatic beta-cell tumours in transgenic mice expressing recombinant insulin/simian virus 40 oncogenes. Nature. 1985; 315:115–122. [PubMed: 2986015]
49. Inoue M, Hager JH, Ferrara N, Gerber HP, Hanahan D. VEGF-A has a critical, nonredundant role in angiogenic switching and pancreatic beta cell carcinogenesis. Cancer Cell. 2002; 1:193–202. [PubMed: 12086877]

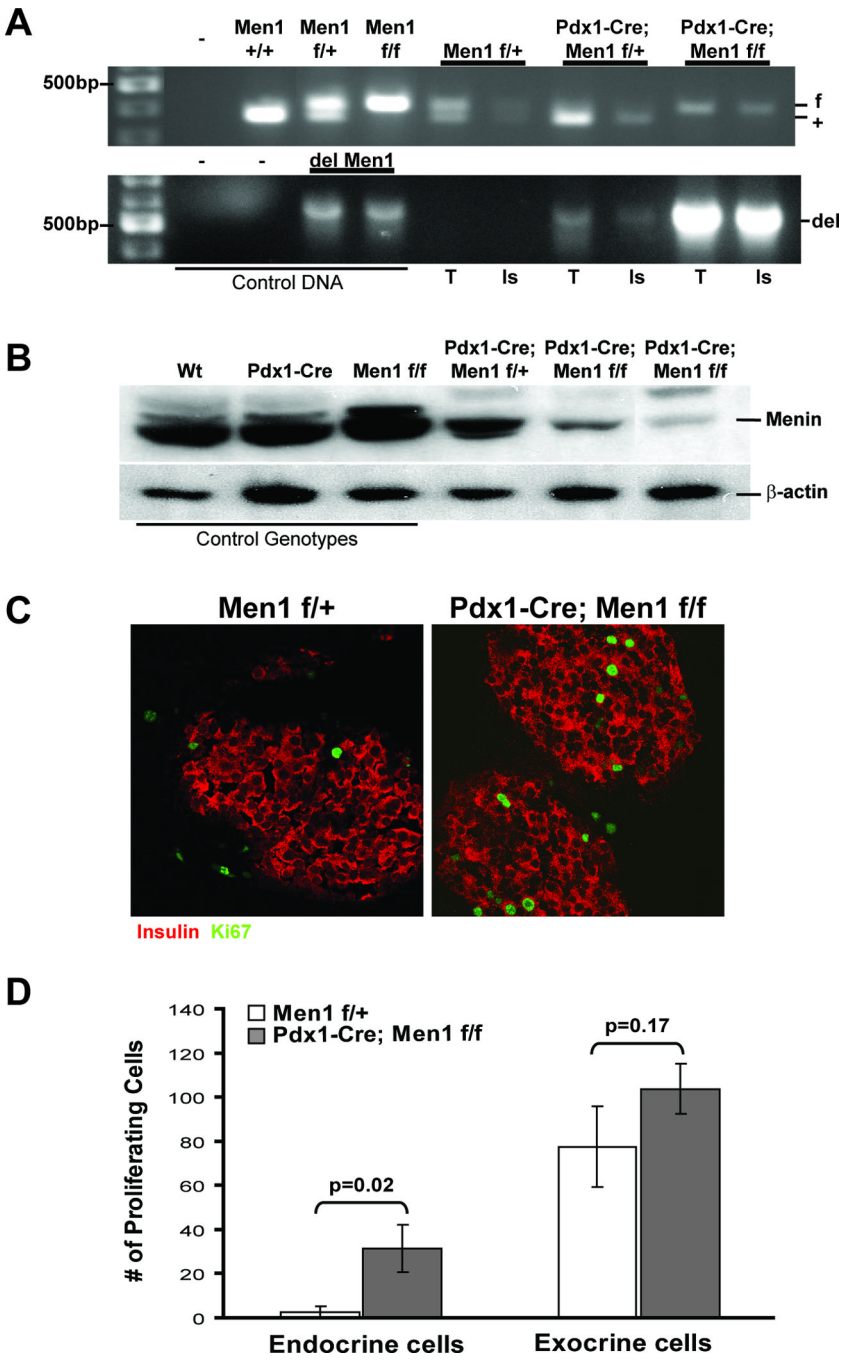

Figure 1. Generation of Pdx1-Cre;Men1 f/f mice

A. Deletion of the *Men1* alleles in mouse pancreas. Genotyping PCR using genomic DNA isolated from pancreas exocrine (T, tissues), and endocrine cells (Is, islet) using laser captured microdissection. Top panel shows the status of *Men1* alleles (f, flox, 430bp; +, wildtype, 380bp), and bottom panel indicates the presence of deleted *Men1* allele (del, 638bp) only in Pdx1-Cre positive pancreas. **B.** Western Blot analysis of menin protein expression (76kDa) in mouse pancreas using total pancreatic protein lysate in a 12-month old cohort. Genotype of each mouse is indicated on top (wt, wildtype), and β-actin (43kDa) is used as loading control. **C.** Immuno-fluorescent staining for insulin (red) and Ki-67

(green) of representative control Men1 f/+ and mutant Pdx1-Cre;Men1 f/f islets of 2–3 month old mice, images are taken at 400×. **D.** Quantification of proliferating cells in endocrine islets or exocrine cells of pancreas in mice at 2–3 month of age. The bar graph represents two different animals of the same genotype, and multiple images were analyzed for each animal. The absolute number of Ki-67 positive proliferating cells was counted within the endocrine and exocrine tissues for each image utilizing the AxioVision software.

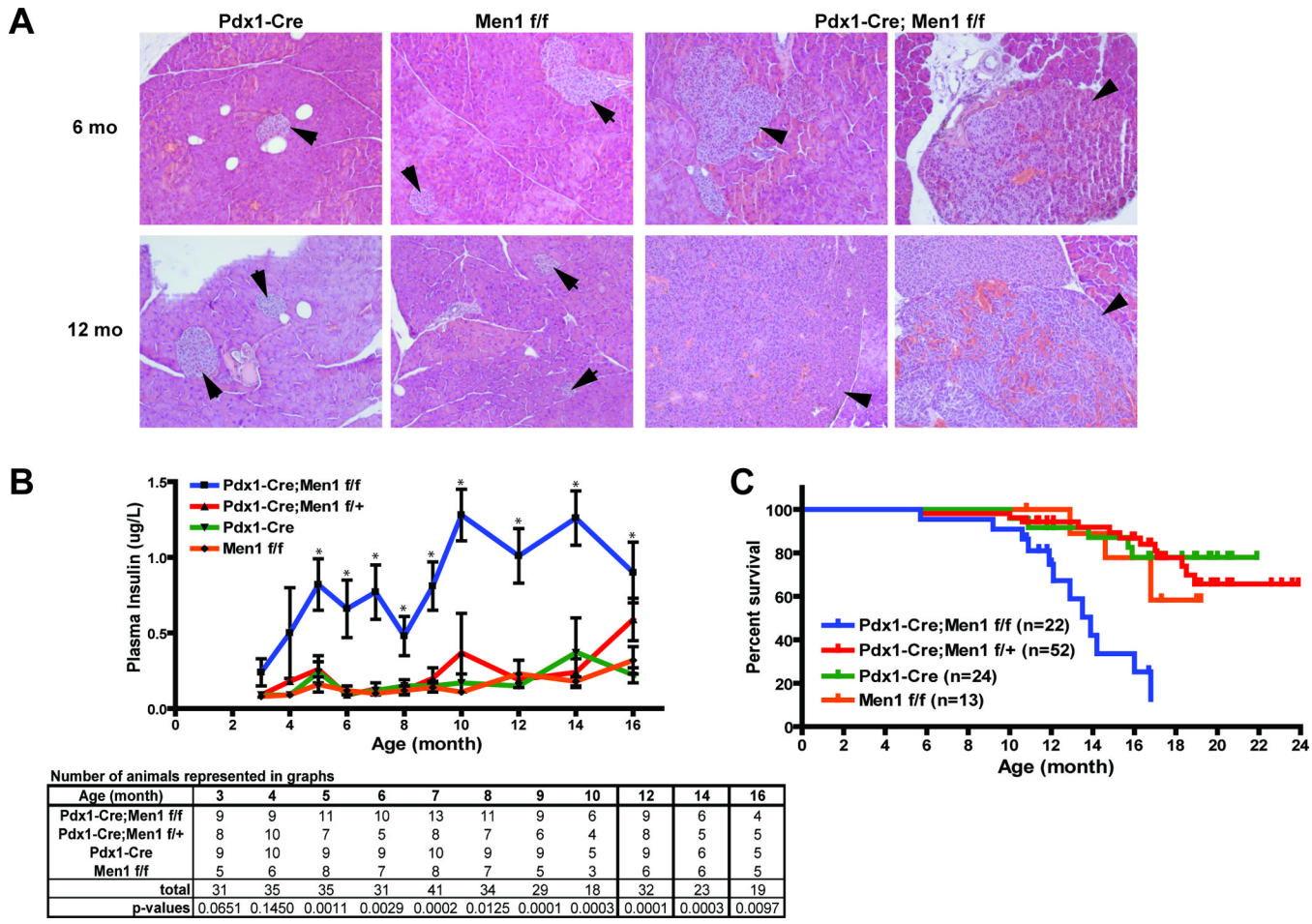

Number of animals represented in graphs

Age (month)	3	4	5	6	7	8	9	10	12	14	16
Pdx1-Cre;Men1 f/f	9	9	11	10	13	11	9	6	9	6	4
Pdx1-Cre;Men1 f/+	8	10	7	5	8	7	6	4	8	5	5
Pdx1-Cre	9	10	9	9	10	9	9	5	9	6	5
Men1 f/f	5	6	8	7	8	7	5	3	6	6	5
total	31	35	35	31	41	34	29	18	32	23	19
p-values	0.0651	0.1450	0.0011	0.0029	0.0002	0.0125	0.0001	0.0003	0.0001	0.0003	0.0097

Figure 2. Histological and physiological analyses of control and mutant Pdx1-Cre;Men1 f/f mouse pancreas

A. H&E staining of representative control Pdx1-Cre;Men1 f/f pancreas and two mutant Pdx1-Cre;Men1 f/f pancreas at 6 and 12 months (mo) of age. Normal islets in control animals are indicated by arrows, while hyperplastic islets and insulinomas filled with blood islands in Pdx1-Cre;Men1 f/f animals are indicated by arrowheads. Images are taken at 200×. **B.** Fasted plasma insulin levels in mice of indicated genotype. Number of animals and p-values analyzed at each time point are shown in table below. **C.** Kaplan-Meier survival curve by genotype. Each tick mark represents the age of a live animal at termination of this study, and the numbers of animals (n) for each genotype are as indicated.

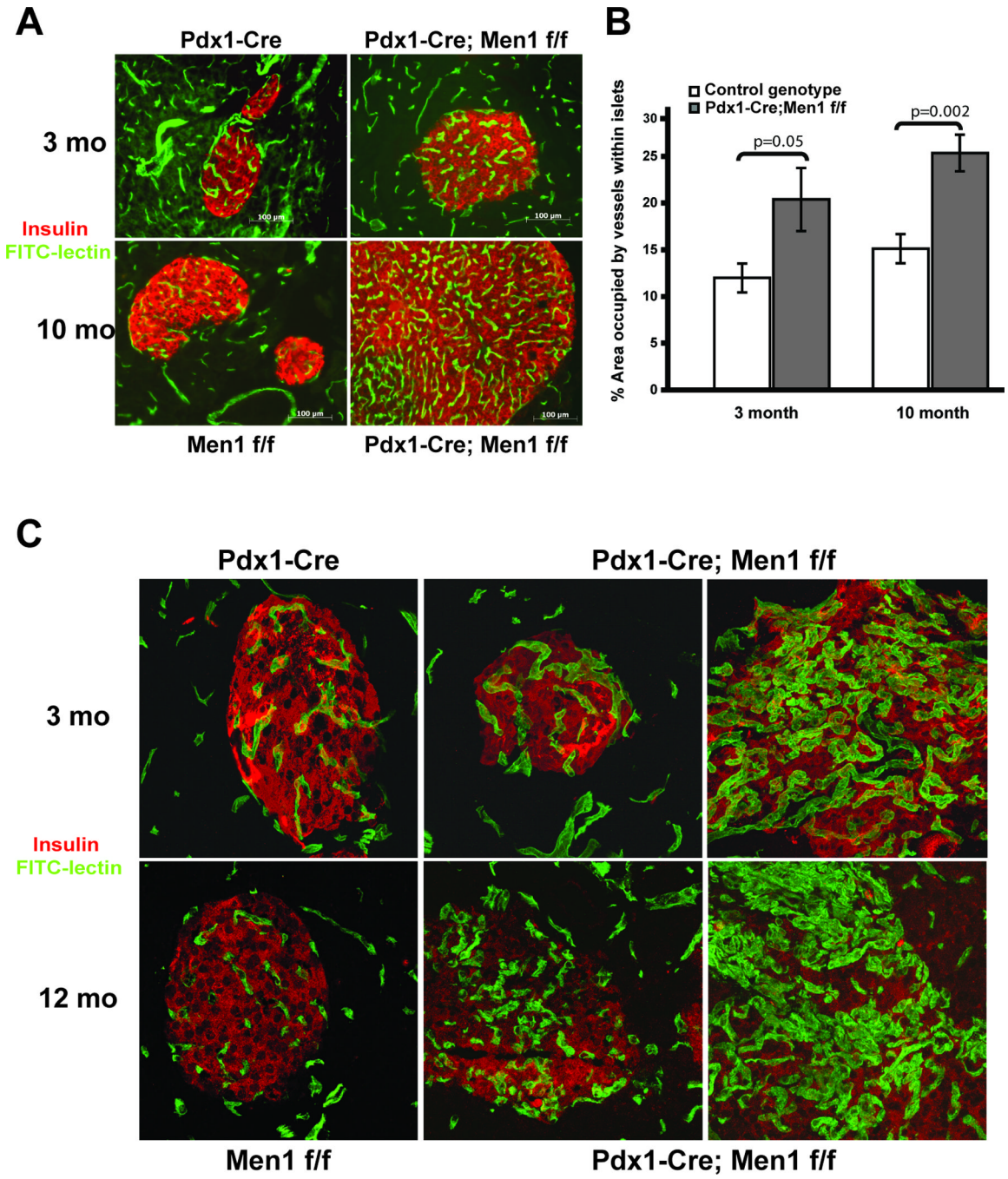

Figure 3. Vascular phenotype in pancreatic islets of Pdx1-Cre;Men1 f/f mice

A. Immuno-fluorescent staining of representative islet vasculature in control Pdx1-Cre, Men1 f/f and mutant Pdx1-Cre;Men1 f/f pancreas at 3 and 10 months of age. Blood vessels are visualized via FITC-lectin injection (green) while pancreatic islets are identified using an anti-insulin antibody (red). **B.** Quantitative analysis of islet vascularity in mouse pancreas of control and mutant genotypes, with two animals in each genotype. **C.** Representative z-stack confocal immuno-fluorescent images of pancreatic islet vasculature in control Pdx1-Cre, Men1 f/f and two mutant Pdx1-Cre;Men1 f/f animals at 3 and 12 months of age. Blood

vessels are visualized via FITC-lectin injection (green) while pancreatic islets are identified using an anti-insulin antibody (red), images are taken at 400×.

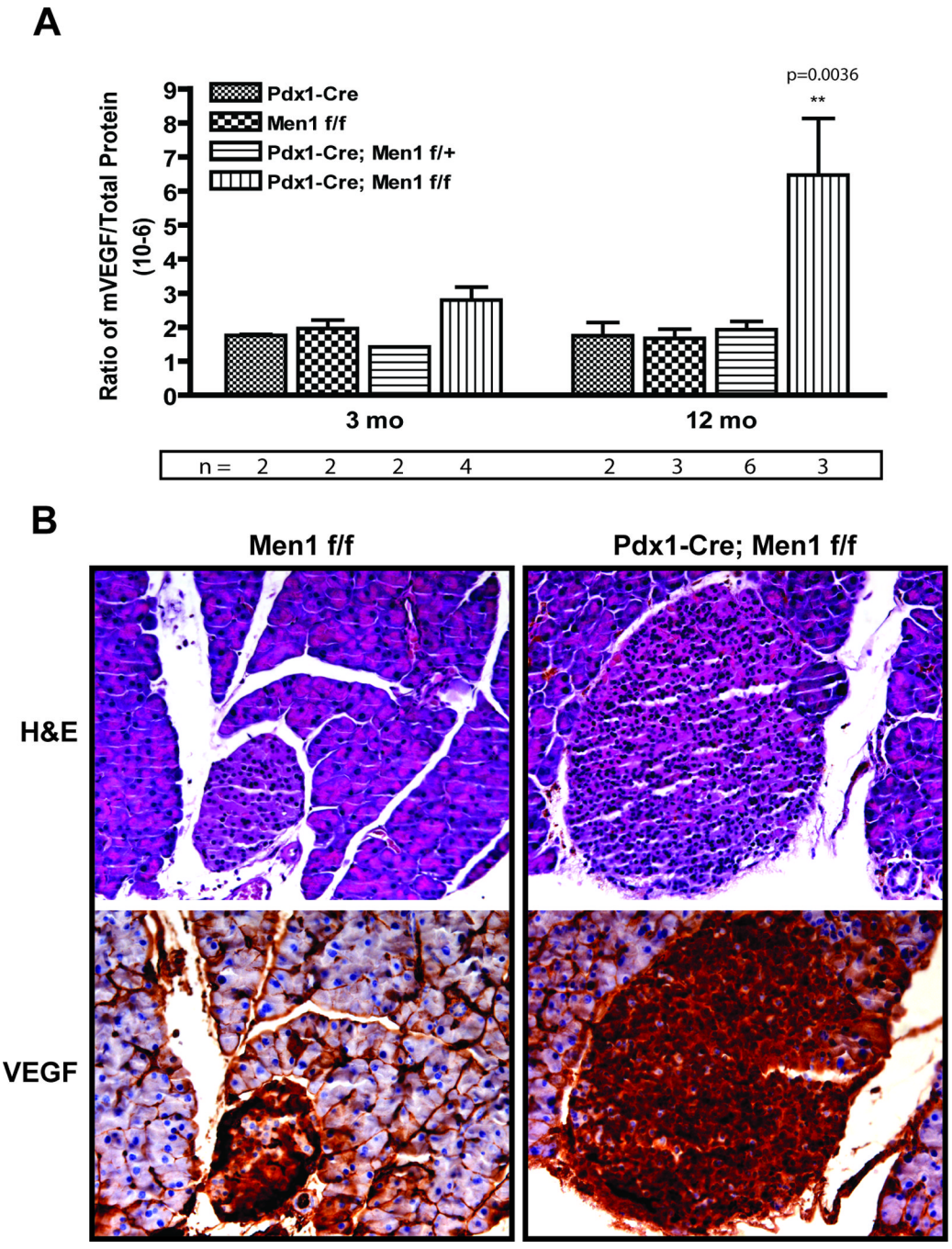

Figure 4. Involvement of VEGF in the insulinomas developed in Pdx1-Cre;Men1 f/f mice

A. VEGF protein expression in mouse pancreas of indicated genotype. Each bar represents the average of multiple animals (n, as shown) for each genotype at two different time points. **B.** Representative immuno-histochemical staining of VEGF in control Men1 f/f and mutant Pdx1-Cre;Men1 f/f mice at 16 months of age. Adjacent H&E section is shown to identify islets. Positive VEGF protein is visualized as dark brown staining, images are taken at 320×.

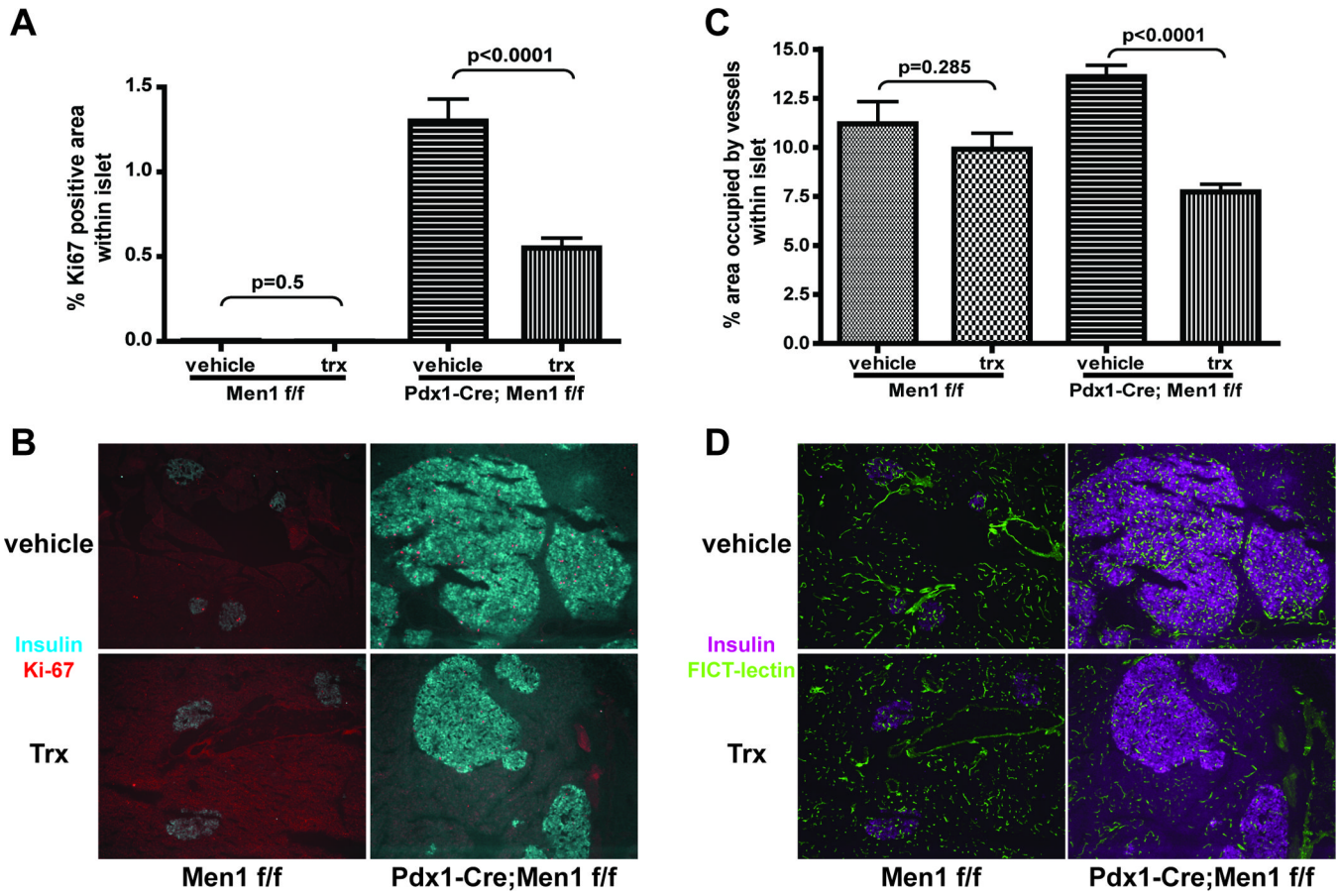

Figure 5. Quantitative analysis of immuno-fluorescent images for percentage of Ki-67 positive areas within islets

(A) and islet vascularity **(C)** in vehicle or sunitinib treated (trx) animals of control Men1 f/f and mutant Pdx1-Cre;Men1 f/f genotypes. Representative images are shown in panel B and panel D. **B**. Ki-67 positive areas and islets are identified using antibodies against Ki-67 (red) and insulin (cyan). Percentage of Ki-67 positive areas within islet are shown to account for differences of islet size between control Men1f/f and mutant Pdx1-Cre;Men1 f/f genotypes. **D**. Blood vessels are visualized via FITC-lectin injection (green) while pancreatic islets are identified using an anti-insulin antibody (magenta). All images are at 100×.

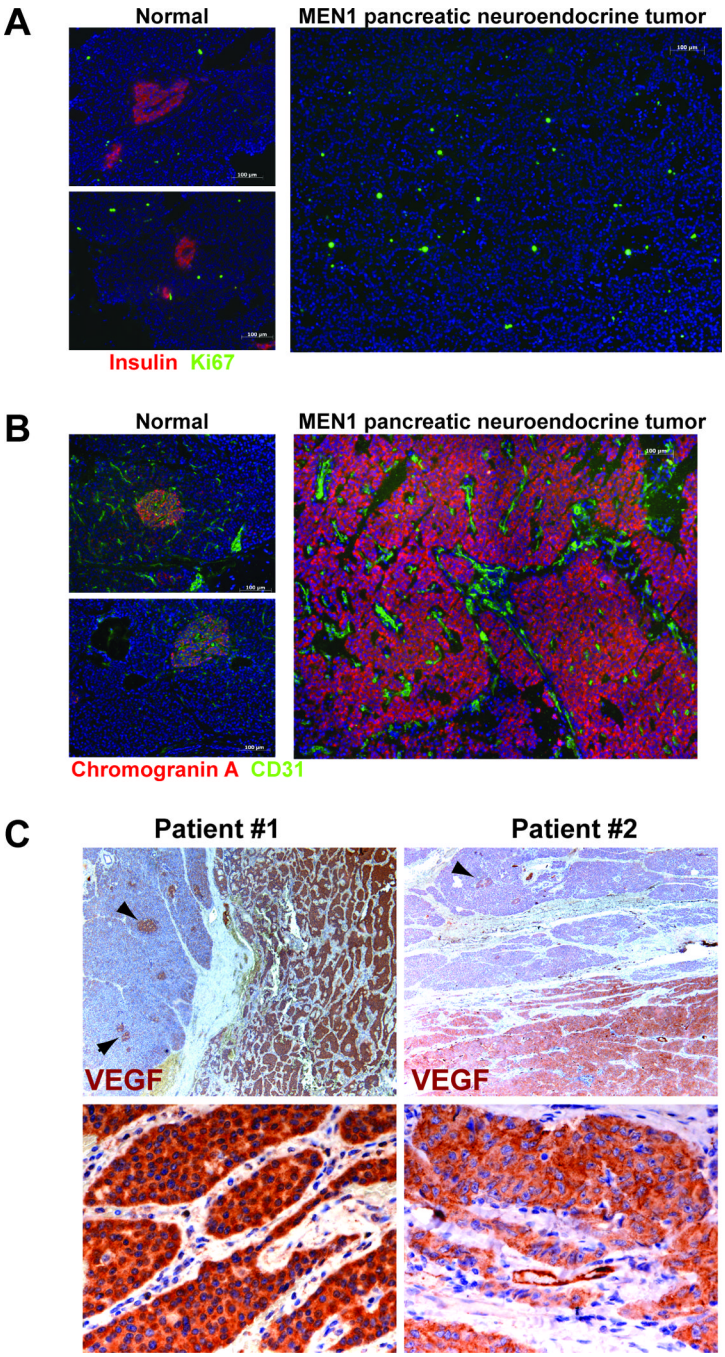

Figure 6. Histological analyses of human MEN1 pancreatic neuroendocrine tumors

A. Pancreatic islets are visualized using an anti-insulin antibody (red), while a Ki-67 antibody identifies proliferating cells (green). A non-functional neuroendocrine tumor is shown; thus, is negative for insulin staining and positive for chromogranin A (shown in panel B). Images are taken at 200×. **B.** Chromogranin A is utilized to identify normal islets and neuroendocrine tumor (red), while CD31 is used to visualize blood vasculature. Images are taken are 200×. **C.** VEGF positive staining is shown as reddish-brown color in two MEN1 patients. Top panels indicate normal islet (arrowheads) adjacent to the tumors (reddish-brown stain) at 40×; whereas bottom panels show only the tumor areas at 500×.